Temperature- and time-resolved X-ray scattering at thin organic films†

Y. Bodenthin,[a] J. Grenzer,[a] R. Lauter,[a] U. Pietsch,[a]* P. Lehmann,[b] D. G. Kurth[b] and H. Möhwald[b]

[a]Institute of Physics, University of Potsdam, D-14415 Potsdam, Germany, and [b]Max-Planck-Institute of Colloids and Interfaces, D-14476 Golm, Germany. E-mail: upietsch@rz.uni-potsdam.de

Multilayers of an Fe(II)-polyelectrolyte-amphiphile complex (Fe-PAC) were investigated simultaneously by energy-dispersive X-ray reflectivity and in-plane diffraction at the bending-magnet beamline at BESSY II. By recording spectra between room temperature and about 348 K with a time resolution of about 60 s, two phase transitions were identified and the respective activation energies were determined. Owing to a fixed geometrical set-up, an energy-dispersive experiment is suitable for measuring X-ray reflectivity and in-plane X-ray diffraction of thin organic films simultaneously. Installed at a bending magnet at BESSY II and using an energy range of $4 < E < 25$ keV, both reflectivity and diffraction spectra can be collected within about 60 s. The performance is demonstrated by temperature- and time-resolved measurements of the phase transition behaviour of multilayers of an Fe-PAC deposited on a silicon support by means of the Langmuir–Blodgett (LB) technique. By measuring the X-ray reflectivity while increasing the temperature, it is shown that the original LB phase is not stable and transforms irreversibly into a liquid-crystalline (LC)-like phase at about 318 K. At the same temperature the in-plane diffraction signal vanishes reversibly, reflecting rotational disorder of the hexagonal arrangement of amphiphilic chains. Its activation energy is determined to be about 1.3 eV. At about 338 K a second irreversible phase transition occurs to another LC phase with smaller vertical layer spacing. This transition is reversible between 329 K and 338 K.

Keywords: energy-dispersive reflectometry; phase transitions; supramolecular chemistry.

1. Introduction

An energy-dispersive experiment makes use of the white energy spectrum provided by a home tube or storage ring in an effective manner. Most of the applications known up to now are focused on diffraction from crystals under extreme conditions, *e.g.* in high-pressure physics (Neuling & Holzapfel, 1992). Early and novel white-beam applications of X-ray reflectivity are based on X-ray tubes or rotational anodes (Bilderback & Hubbard, 1982; Chason *et al.*, 1992; Roser *et al.*, 1994; Metzger *et al.*, 1994; Mahler *et al.*, 1995; Wallace & Wu, 1995; Windover *et al.*, 2000). An energy-dispersive X-ray reflectometer is partially installed at beamline BL20B at the Taiwan Light Source (Lee *et al.*, 1998); another was in use at the wavelength shifter of BESSY I (Neissendorfer *et al.*, 1999).

At BESSY II the white-beam experiment installed at the bending magnet is applied for X-ray reflectivity and grazing-incidence diffraction. It exploits the exponentially decaying hard tail of the 1.7 GeV BESSY emission spectrum in the range $4 < E < 30$ keV. The incident beam is manipulated by different slits without passing through any further optical element before it strikes the sample aligned on the goniometer. Using a typical slit width of 0.1 mm × 1 mm and a beam current of 100 mA, the usable incident beam intensity is of the order of 10^{10} counts s^{-1}, which is sufficient to perform time-resolved experiments. Time- and temperature-resolved specular (Englisch *et al.*, 1998) and diffuse reflectivity (Pietsch *et al.*, 2001) and in-plane grazing-incidence diffraction from thin films (Grenzer *et al.*, 2000) are realistic applications of this set-up. In the present paper we demonstrate its capability by simultaneous measurement of the in-plane and out-of-plane lattice spacing of thin organic films during annealing. In particular, we inspect the phase-transition behaviour of Fe-polyelectrolyte-amphiphilie complexes (Fe-PAC) deposited as multilayers by means of the Langmuir–Blodgett (LB) technique.

2. Sample preparation

The molecular system used in the experiment is sketched in Fig. 1. By self assembly of 1,4-bis(2,2′:6′,2-terpyridin-4′-yl)benzene ligands with Fe(II) ions, a linear positively charged macromolecule (1) was formed with a separation length of 1.6 nm between adjacent metal ions (Schütte *et al.*, 1999; Kurth *et al.*, 2000). Treatment of an aqueous solution of (1) with 1.5 equivalents of the 23 Å-long amphiphile dihexadecylphosphate (DHP) dissolved in chloroform resulted in the formation of Fe(II)-PAC (2). 2.45 mg of the purified powder of (2) were dissolved in 10 ml chloroform and 300 µl of the solution were spread onto distilled water (USF Seral, 18.2 MΩ cm at 298 K) in a Langmuir trough. Subsequent transfer of monolayers on a hydrophilic silicon substrate resulted in multilayer films. Using a constant surface pressure of 40 mN m^{-1} and a dipping speed of 6 mm min^{-1} the transfer ratio was 0.95 ± 0.05 for up- and down-stroke deposition.

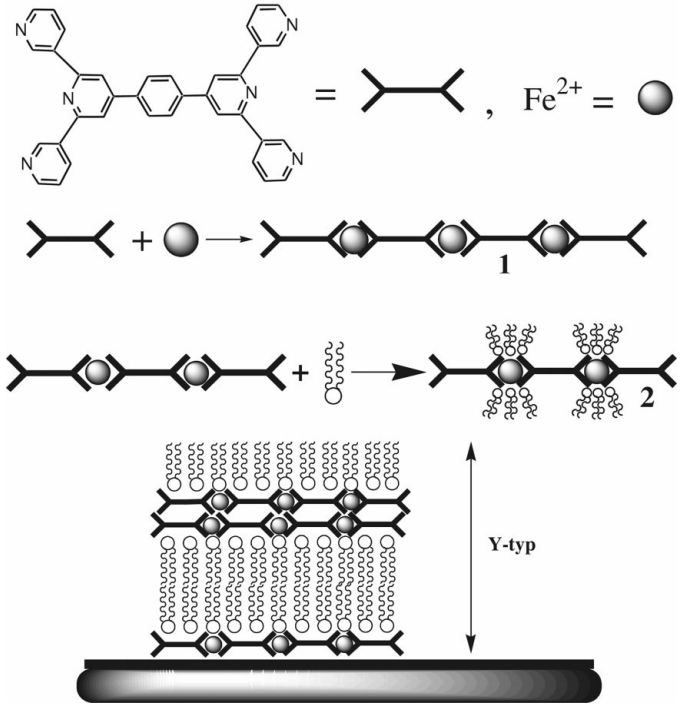

Figure 1
Sketch of the molecular system used in the experiment.

† Presented at the 'ESF Exploratory Workshop on Time-Resolved Investigations with Neutrons and X-rays (TINX)' held in Berlin, Germany, in September 2001.

3. Experimental realisation

The experimental set-up used is similar to that published recently (Neissendorfer *et al.*, 1999) and is shown schematically in Fig. 2. The incident beam is guided in-vacuum up to the exit window of size 0.1 mm × 1 mm and hits the sample at a fixed angle α with respect to the sample surface and is recorded at the detector angle 2α. As a detector we used a silicon drifted diode (Röntec), which is linear in response up to photon numbers of about 2×10^5 counts s^{-1} with an energy resolution of about 250 eV (Röntec, 2002). Additional advantages are the low electronic background (<0.1 count s^{-1}) and the almost uniform detector efficiency within the energy range of interest. Nevertheless, the totally reflected intensity depends on α and has to be attenuated. The absorber thickness determines the onset of the measurable reflectivity spectrum. To tune the incident intensity we used an absorber box hosting a number of thin aluminium plates of thicknesses 0.1, 0.2, 0.4, 0.8, 2, 4, 8 and 15 mm, providing attenuation by a factor $I/I_0 = 0.27, 0.07, 5 \times 10^{-3}, 3 \times 10^{-5}, 4 \times 10^{-12}, \ldots$ at 6 keV but 0.8, 0,6, 0.4, 0.15, 0.01, 1×10^{-4}, 1×10^{-8}, ... at 15 keV, respectively. Increasing the thickness of the absorbers provides information on the sample which appears at higher energies. Fig. 3(*a*) shows the reflectivity spectra $I(E)/I_0(E)$ as a function of energy recorded at different α from a 15-layer-thick LB film. We used the 0.1 mm absorber for $\alpha = 1^\circ$ and $\alpha = 1.5^\circ$ but no absorber for $\alpha = 2^\circ$. Therefore the onset of the latter spectrum appears at 3 keV, compared with 5 keV for the other two. For better clarity the intensities are plotted with an offset of about 10%. In Fig. 3(*b*) the same curves are plotted *versus* q_z, given by

$$q_z \simeq \alpha E, \tag{1}$$

making use of $4\pi e/hc \simeq 1/(\text{Å} \times \text{keV})$, where α is measured in radians. The quantity q_z is given in Å^{-1} when E is given in keV (Neissendorfer *et al.*, 1999; Holy *et al.*, 1999). Considering the total film thickness D and the vertical lattice spacing d, thickness oscillation maxima and Bragg peaks, respectively, appear at energies

$$E_n = nhc/(2\Delta \sin\alpha), \tag{2}$$

using $\Delta = D$ or d. n is the respective reflection order. Whereas in angular space the peak distances change with $1/\alpha$, the period of oscillation is constant in E-space (q-space) and depends on film thickness only. The measured spectra shown in Fig. 3 are normalized by the incident spectrum. Modified by the absorbers in use, the latter is approximated by a function (Neissendorfer *et al.*, 1999)

$$I_0(E) \simeq \exp(-aE)\exp(-b/E^3). \tag{3}$$

The second exponential in (3) considers the energy-dependent absorption by the beryllium windows, the absorber foils and air. The first exponential describes the decay of the incident beam, where a and b are fitting parameters. After normalization, the measured energy-dispersive spectra can be treated similarly to a reflectivity curve $I(q_z)q_z^4$ measured with monochromatic radiation after normalization to Fresnel's reflectivity (Holy *et al.*, 1999). The similarity of both experiments has been demonstrated by Geue *et al.* (2000). As shown by Holy *et al.* (1999), the experimental resolution is

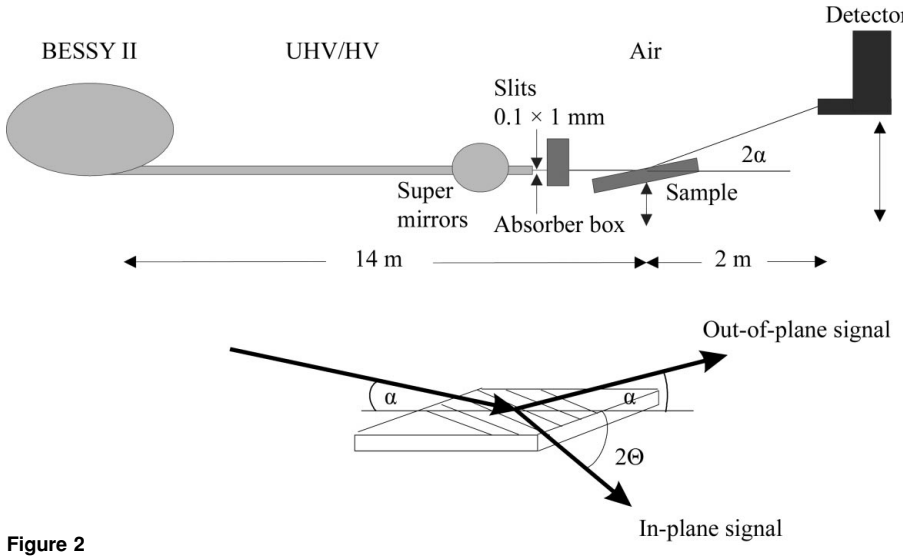

Figure 2
Schematic sketch of the experimental set-up used at BESSY II.

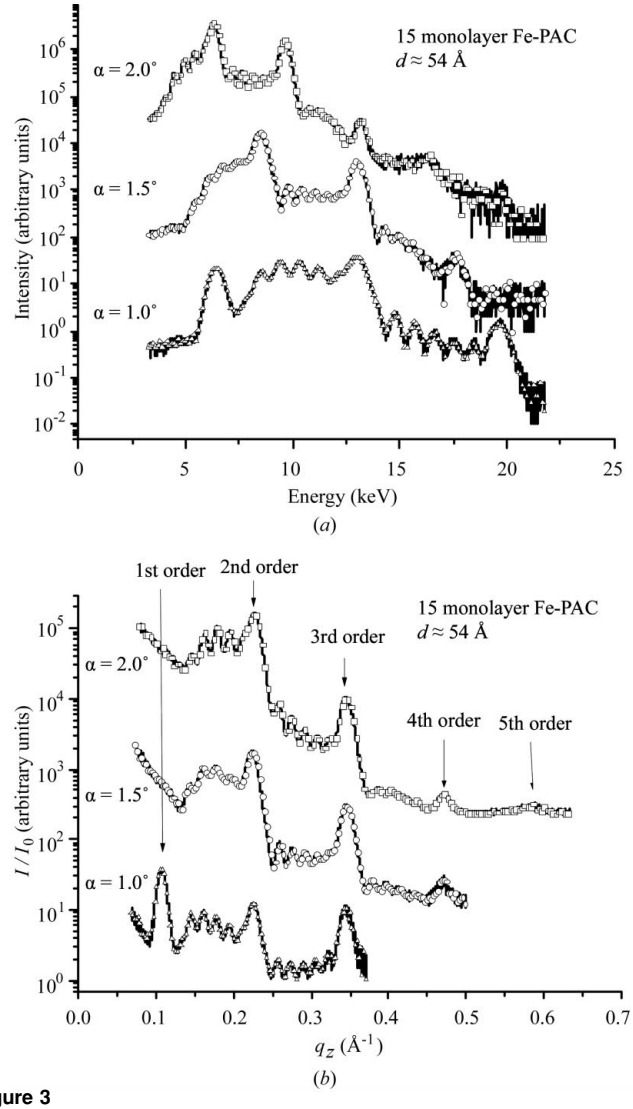

Figure 3
Energy-dispersive reflectivity of a 15 monolayer film recorded at different incident angles displayed (*a*) as a function of energy and (*b*) after re-scaling in q_z. The curves are separated artificially by an offset of 100. The absorber thickness was 0.1 mm for $\alpha_i = 1^\circ$ and 1.5°; no absorber was used for $\alpha_i = 2^\circ$.

a function of energy. The increasing peaks width *versus* energy in Fig. 3(*a*) is partially due to this effect.

Fig. 4 shows several reflectivity spectra recorded at different temperatures at $\alpha = 1^\circ$. They are selected from a series of spectra collected over a temperature ramp of about 120 s K^{-1}. The recording time of each spectrum was 60 s. Above 318 K the shape of the spectrum changes, indicating a phase transition from the LB phase with $d_{LB} = 56$ Å into a liquid-crystalline (LC) phase with $d_{LC} = 52$ Å. The phase transition is irreversible because d_{LB} cannot be restored after cooling the sample below 318 K. Nevertheless, the entire film structure has remained intact and the Kiessig fringes remain visible. The latter measure the total thickness, which corresponds to 15 monolayers. The LC phase seems to be stable up to about 338 K. Between 318 K and 338 K the lattice spacing continuously changes reversibly to $d_{LC} = 50$ Å. Above 338 K the film completely reorganizes its structure. Kiessig fringes are no longer visible, the Bragg peaks of the LC phase vanish, but new Bragg peaks appear. The latter peaks have different peak widths indicating simultaneous appearance of stacks of different spacing and number of monolayers. At 343 K the peaks at $q_z = 2\pi/d = 0.136$ Å^{-1} and $q_z = 4\pi/d = 0.27$ Å^{-1} correspond to a layer spacing of the high-temperature (HT) phase of $d_{HT} = 46$ Å.

Fig. 5 shows in-plane diffraction spectra recorded at different temperatures. The counting time was 120 s each. Here the incident beam strikes the sample surface at a shallow angle of incidence $\alpha = 0.2^\circ$. The beam is reflected and diffracted simultaneously at in-plane lattice planes created by the lateral arrangement of amphiphilic molecules. Depending on the arbitrarily chosen in-plane diffraction angle ($2\Theta \simeq 20^\circ$) the diffracted Bragg peak appears at an energy

$$E_{in} = 2\pi/(\Theta q_{x,y}), \tag{4}$$

whereas $q_{x,y} \simeq \Theta E$, similar to equation (1). For the present case, the large peak at $q_{x,y} = 1.5$ Å^{-1} corresponds to a lattice spacing of $d_{in} = 4.2$ Å, which is typical for a hexagonal arrangement of amphiphilic molecules. In an energy-dispersive set-up the critical angle α_c is a function of energy (Neissendorfer *et al.*, 1999). For $2\Theta \simeq 20^\circ$ the main peak appears close to 8 keV where the critical angle of silicon substrate is $\alpha_c \simeq 0.25^\circ$. Thus, $\alpha = 0.2^\circ = 0.8\alpha_c$ corresponds to similar conditions as used typically in angular-dispersive experiments (Tippmann-Krayer *et al.*, 1992; Barberka *et al.*, 1994). It guarantees an information depth of the order of the film thickness. No other features appeared outside the energy range shown in Fig. 5. The width of the peak at $q_{x,y} = 1.5$ Å^{-1} is mainly determined by the correlation length L of laterally molecular order. After correction for the experimental broadening, L is estimated to be 70 ± 1 Å, which corresponds to about 18 next-neighbour distances. Another peak appears at $q_{x,y} = 1.1$ Å^{-1} reflecting the K-fluorescence ($E = 6.4$ keV) of the Fe(II) atoms in the sample, which allows EXAFS investigations of the Fe(II) next-neighbour coordination (Bodenthin *et al.*, 2001). As shown, the Bragg peak intensity decreases for increasing temperature. It vanishes at about $T = 318$ K, *i.e.* at a temperature equal to the first phase transition observed in the reflectivity measurement. In contrast to the reflectivity channel, the in-plane signal reappears at the same energy if the sample is cooled below $T = 318$ K. The second phase transition above $T = 338$ K is not accompanied by the appearance of a new in-plane Bragg peak.

The kinetics of both phase transitions were studied by time-dependent measurements (not shown here). To do this, spectra were recorded at a fixed temperature close to the phase transition temperature and the decay of the peak intensity was recorded as a function of time. After correction by the storage-ring intensity this decay gives a time constant. Next, the temperature is slightly increased and the time constant is measured again. A plot of the reciprocal time constants *versus* $1/T$ (Englisch *et al.*, 1998) provides the activation energies $E_{C1} = 1.3 \pm 0.2$ eV for the first phase transition at 318 K and $E_{C2} = 1.2 \pm 0.3$ eV for the second transition at about 338 K.

4. Discussion

The present experiment demonstrates the capability of the energy-dispersive set-up for the determination of three-dimensional structural phase transitions in supramolecular multilayers. Even for temperature-dependent experiments the simultaneous recording of the reflected and diffracted intensity guarantees that both experi-

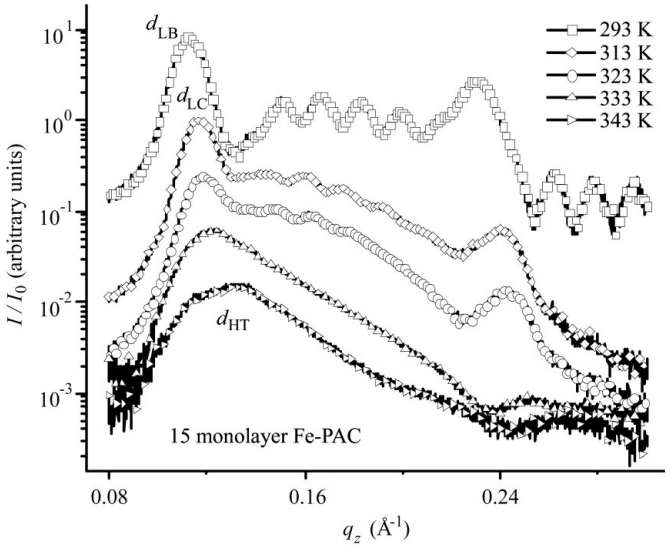

Figure 4
Reflectivity spectra at $\alpha = 1^\circ$ recorded at different temperatures. The curves are artificially separated from each other.

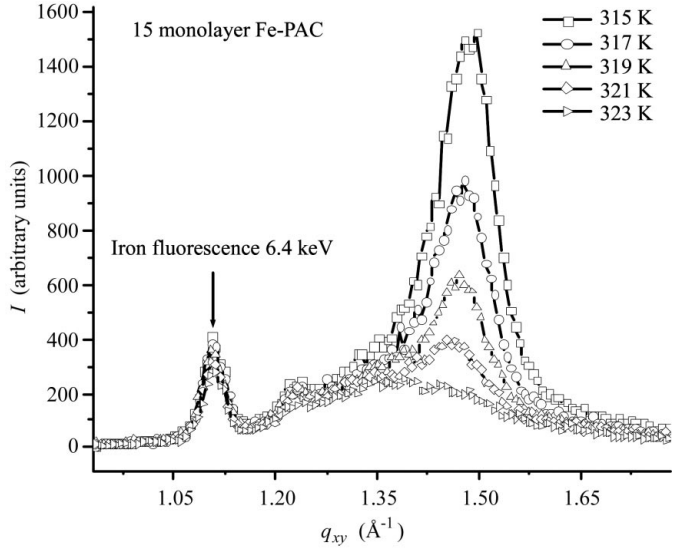

Figure 5
In-plane diffraction spectra recorded at different temperatures.

ments are carried out under identical conditions, which is necessary to identify the nature of the indicated phase transitions. The present investigations were performed at $\alpha = 1^\circ$ first for reflectivity and at $\alpha = 0.2^\circ$ thereafter for grazing-incidence diffraction. Because both experiments were realised under equal outer conditions, *i.e.* the same temperature, same temperature controller, same environment, and so forth, it is evident that the in-plane signal changes at equal temperature as observed in reflectivity. Because the in-plane signal is restored below 318 K, the respective phase transition can be described by a transition from the ordered LB multilayer into an LC phase with rotational disorder of the amphiphilic chains. The change in layer spacing can be explained by a molecular tilt of the alkyl chains of the amphiphiles with respect to the surface normal, which is about 21° at the phase-transition temperature but increases to 26° close to 323 K. The second (irreversible) phase transition is associated with a loss of vertical correlation. The layer spacing has changed and several additional *d*-values appear simultaneously. The nature of this high-temperature phase has not yet been evaluated. The increase of the peak widths corresponds to vertically correlated stacks of two to four monolayers. One possible explanation is a spatial rearrangement of monolayers within the multilayer stack. Whereas the LB and LC phases are stacked vertically in a Y-conformation, *i.e.* the Fe-PAC monolayers are ordered as alkyl-chain–polyelectrolyte–polyelectrolyte–alkyl-chain, the high-temperature phase might be stacked in the order alkyl-chain–polyelectrolyte–alkyl-chain. This would require a subsequent lateral shift of each second Fe-PAC unit in one direction by half of the in-plane lattice spacing. Another model might be a phase transition into a three-dimensional hexagonal phase of Fe-PAC molecules, as suggested by powder diffraction data (Kurth *et al.*, 2002).

The authors thank BESSY for the possibility of installing the beamline, and DFG and MPI-KGF for financial support.

References

Barberka, T. A., Höhne, U., Pietsch, U. & Metzger, T. H. (1994). *Thin Solid Films*, **244**, 1061–1066.

Bilderback, D. H. & Hubbard, S. (1982). *Nucl. Instrum. Methods*, **195**, 85–95.

Bodenthin, Y., Pietsch, U., Kurth, D., Lehmann, P., Möhwald, H., Erko, A. & Fieber-Erdmann, M. (2001). *BESSY Annual Report 2001*. BESSY, Berlin, Germany.

Chason, E., Mayer, T. M., Rayne, A. & Wu, D. (1992). *Appl. Phys. Lett.* **60**, 2353–2355.

Englisch, U., Penacorada, F., Samoilenko, I. & Pietsch, U. (1998). *Physica B*, **248**, 258–262.

Geue, Th., Grenzer, J., Mukherjee, M., Sanyal, M. K., Pucher, A. & Pietsch, U. (2000). *BESSY Annual Report 2000*, pp. 231–232. BESSY, Berlin, Germany.

Grenzer, J., Pucher, A., Geue, Th., Symietz, ch., Neissendorfer, F. & Pietsch, U. (2000). *BESSY Annual Report 2000*, pp. 233–234. BESSY, Berlin, Germany.

Holy, V., Pietsch, U. & Baumbach T.(1999). *High-Resolution X-ray Scattering from Thin Films and Multilayers*, Springer Tracts in Modern Physics, Vol. 149. Berlin: Springer.

Kurth, D. G., Lehmann, P. & Schütte, M. (2000). *Proc. Natl Acad. Sci.* **97**, 5704–5707.

Kurth, D. G., Meister, A., Thünemann, A. & Förster, G. (2002). *Proc. Natl. Acad. Sci USA*. Submitted.

Lee, C. H., Hwang, C. S., Tseng, P. K., Yu, K. L., Tseng, H. C., Su, W. C., Chen, R. J., Lin, T. L. & Chang, S. L. (1998). *J. Synchrotron Rad.* **5**, 512–514.

Mahler, W., Barberka, T. A., Pietsch, U., Höhne, U. & Merle, H.-J. (1995). *Thin Solid Films*, **256**, 198–205.

Metzger, T. H., Luidl, C., Pietsch, U. & Vierl, U. (1994). *Nucl. Instrum. Methods*, A**350**, 398–405.

Neissendorfer, F., Pietsch, U., Brezesinski, G. & Möhwald, H. (1999). *Meas. Sci. Techn.* **10**, 354–361.

Neuling, H. W. & Holzapfel, W. B. (1992). *High Press. Res.* **8**, 655–660.

Pietsch, U., Grenzer, J., Geue, Th., Neissendorfer, F., Brezsesinski, G., Symietz, ch., Möhwald, H. & Gudat, W. (2001). *Nucl. Instrum. Methods Phys. Res. A*, **467/468**, 1077–1080.

Röntec (2002). Röntec Holding AG homepage, http://www.roentec.com.

Roser, S. J., Felici, F. & Eaglesham, A. (1994). *Langmuir*, **10**, 3853–3856.

Schütte, M., Kurth, D. G., Linford, M. R., Cölfen, H. & Möhwald, H. (1999). *Angew. Chem. Int. Ed. Engl.* **38**, 2547–2550.

Tippmann-Krayer, P., Kenn, R. M. & Möhwald, H. (1992). *Thin Sold Films*, **210**, 577–583.

Wallace, W. E. & Wu, W. L. (1995). *Appl. Phys. Lett.* **67**, 1263–1265.

Windover, D., Lu, T.-M., Lee, S. L., Jin, C. & Lee, W. (2000). *Appl. Phys. Lett.* **76**, 158–160.

 Received 23 January 2002 • Accepted 29 April 2002